Fermilab

TM-1205
1620.000

ELECTRICAL AND MAGNETIC PROPERTIES OF THE ENERGY SAVER CORRECTION ELEMENTS*

M. Johnson, A. McInturff, R. Raja, and P. Mantsch

August 1983

*Submitted to the 12th International Conference on High Energy Accelerators, August 11-16, 1983, Fermilab, Batavia, IL 60510.

Electrical and Magnetic Properties of the Energy Saver Correction Elements

M. Johnson, A. McInturff, R. Raja, and P. M. Mantsch
Fermi National Accelerator Laboratory*
P.O. Box 500
Batavia, Illinois 60510

Abstract

The lattice of the Fermi National Accelerator Laboratory's Energy Saver/Doubler contains a group of superconducting correction windings associated with each quadrupole. These are housed in an element referred to as a "spool"[1]. There are 192 spools in the ring plus 12 special power spools which contain the main buss 5000 ampere power input as well as correction elements. There will be constructed and tested 290 spools, including spares of each of the eight different types. There have been 266 individual spools tested to date. The spools were tested for A) magnetic field quality, harmonic moments, transfer constants and coil angles, B) high voltage integrity, C) critical transport current, and D) cryogenic operating characteristics (i.e. heatloads, thermometry calibration checks, etc.) Data are summarized for 318 cryogenic tests and magnetic field quality of the 266 different spools, which contain 1614 correction magnet coils.

Introduction

The eight different Energy Saver/Doubler spool types are designated by the notation TSA-000 (Tevatron Spool Type "A", serial number 000). The different types are listed in Table I. There are four categories of correction packages[2], DSQ (Dipole, Sextupole and Quadrupole); OSQ (Octupole, Sextupole and Quadrupole); DDQ (Dipole Horizontal, Dipole Vertical and Quadrupole); and DD (Dipole Horizontal and Dipole Vertical).

TABLE I

SPOOL CORRECTION ELEMENTS SERIES

SPOOL TYPE	DSQ COILS (UP) INNER	MID	OUTER	OSQ COILS (DOWN) INNER	MID	OUTER
		DSQI				
A	2P	6P	4P	NONE		
		DSQII				
B	S-2P	6P	4P	NONE		
		DSQI		OSQI		
C	2P	6P	4P	8P	S-6P	S-4P
		DSQII		OSQI		
D	S-2P	6P	4P	8P	S-6P	S-4P
		DSQI		OSQII		
E	2P	6P	4P	8P	6P	4P
		DSQII		OSQII		
F	S-2P	6P	4P	8P	6P	4P
		DSQI		OSQIII		
G	2P	6P	4P	8P	6P	S-4P
		DDQ COILS				
		DDQI				
H	2P	S-2P	4P	NONE		
		DDI				
Low "β"		2P	S-2P			

S-Skew - Notes: 2P-Normal Dipole (Horizontal Bend)

*Operated by Universities Research Inc., under contract with the U.S. Dept. of Energy.

An arbitrary magnetic field in two dimensions can be represented as:

$$B = \sum_k i\, G_k\, W^{*\,k-1}$$

where $W=x+iy$, $i=\sqrt{-1}$ and G_k is the harmonic amplitude for Pole 2k: k = 1 for a Dipole, 2 for a quadrupole, etc. G is dependent on parameters such as magnetic length and excitation current. This dependence can be removed by defining the harmonic moment as:

$$M_k = G_k/C_p R_o$$

Here G_p is the harmonic amplitude of the primary pole (the pole determined) by the coil configuration), G_k is the amplitude of any other pole and R_o is a reference radius which is 1 inch. If k = 1 and P = 2, M would be the quadrupole field present in a sextupole coil. Since G_k is in general complex, M_k is also complex. The normal harmonic amplitude is defined as the real part of M and the skew harmonic amplitude is defined as the imaginary part.

The primary magnetic field measurement was at room temperature with cross checks at low temperature. The magnetic field is measured by a Morgan coil connected to a lock-in amplifier. The Morgan coil has two sets of windings for poles two through eight. The second set is displaced by $\pi/2k$ radians from the first set (2k is the pole number) so one set measures the normal harmonics and the other set measures the skew harmonics. To make a measurement, the magnet coil is powered at low current (a few hundred milliamps) by an 11 hertz oscillator and a Morgan coil is rotated through one revolution in 64 steps. At each step both the driving current and the Morgan coil voltage are measured. The harmonic amplitudes are determined by a Fourier transform of the data. In order to save time, all of the Morgan coils except the one corresponding to the primary pole of the magnet are connected in series. The individual harmonic amplitudes are then determined by Fourier analysis.

Three elements in a given coil package means that there are four possible polarity combinations and an infinity of Lorentz force patterns (vector cross-products of currents and fields to obtain the resulting forces) as the coils are ramped. Each coil package must operate in all four polarity combinations at the maximum operating current without quenching.

The Tevatron spool types B, D, and F contain pairs of "safety" leads which will carry a 5000A current for a short time to bypass a quenching string of main magnets so the machine may be ramped down without depositing the stored energy of the entire magnet ring into the cryogenic environment. The spools also contain two carbon resistors which act as low temperature thermometers for cryogenic monitoring of the liquid helium. The thermometer calibration is cross checked in the assembled spool. An insulating vacuum compartmentalizing barrier and beam tube vacuum measuring ports, are also located in the spools. The main buss quench stopper and associated voltage taps (2), are located in the single phase helium box of the spool. The function of the quench stopper is to prevent a quench from moving from one cell to another

along the main buss or starting at a safety lead. Many of the, as yet, only partially understood problems of operating a superconducting accelerator will be overcome by the versatility and performance range of the correction coil packages.

Performance

The typical cold magnetic field values are given in Table II. The specifications and procedure for spool tests of electrical and cryogenic performance are given in Ref. 3.

Table II
Magnetic Field Strength And Inductance*
I (Coil) = 50 Amps
Measurement Radius = 2.54 cm

	D	S	Q	O	S	Q	D	D	Q	D	D
∫Bdl T-m	.475	.157	.19	.08	.112	.19	.475		.19	.712	.685
B T	.62	.19	.25	.11	.15	.25	.62	73	25	1.05	.998
L mh	755	603	489	221	390	489	755	981	489	1600	2848

Figures 1 to 6 show ∫Bdl histograms at 11 Hz for various coils used in the spool pieces. The spread in the transfer constant data is the result of manufacturing error and long term drift in the measuring apparatus. The latter can be corrected (to about the 0.5% level) by fitting the transfer constants of all the coils in a spool piece to a standard set of values. Since measuring system drift will affect all coils equally, any deviations from the fit will represent manufacturing errors. The deviations from the fitted data appear in Figures 1-6.

Figures 7 and 8 show the transfer constant measured as a function of frequency at 4.2K for Spool 230 and the upstream part of Spool 157. The data from 5hz and up was taken with apparatus similar to that used for normal room temperature measurements. The zero frequency data was obtained by powering the magnet coil (50 Amps) at full current and then rotating the Morgan coil at constant angular velocity. The Morgan coil signal was amplified by a linear amplifier and integrated with a computer. The room temperature point at 11 Hertz is also plotted. The agreement between the two measurement systems is quite good.

A simple eddy current model of these coils[5] shows that the Morgan coil signal that is in phase with the driving signal has the following form:

$$T = T_0/\sqrt{1 + \omega^2 t^2}$$

where To is the value of the transfer constant at zero frequency, ω is the driving frequency, and t is the time constant for the eddy current circuit. The solid lines in Figures 7 and 8 are the best fit to the data. The "t" can also be determined by measuring the ratio of the in-phase to the 90 degree out- of-phase signal with a lock-in amplifier. These results are summarized in Table III. The model appears to be correct to first order (factor of two).

All the coils of a package, at 4.6K, are individually powered to 75 A. They are then powered in various polarity permutations, a maximum current of 60 amperes initially in each element. Qualification means that no element quenches during these polarity permutations at the qualifying current.

There are 77 electrical measurements made on the typical spool, not including superconducting measurements or approximately 25,000 measurements have been taken. (This number does not include those taken by "Quality Control" during fabrication).

TABLE III

Eddy Current Time Constant (10^{-3}) Sec.

	Fit To Transfer Constant Data	InPhase/Out of Phase Signal From Lock-in Amplifier
Spool 230		
Quadrupole	4.2	2.5
Dipole	7	3.7
Sextupole	1.9	.85
Octupole	1.2	1.6
Spool 157		
Quadrupole	6.1	3.7
Dipole	9.1	4.2
Sextupole	3.9	3.0

The summary of the test results for 319 spool tests were: 16 spools failed the high voltage insulation test between correction coils or correction coil to ground; 16 spools failed the high voltage insulation test between main (5000 A) busses or to ground; 31 coils out of 1614 individual coils tested failed to qualify at operational superconducting current, (because of a large redundancy of coils in the spools only 12 spools were rejected). During the 40 Spool Piece Test Facility runs completed, there have been 5,090 quenches or 3.15 quenches per correction magnet which can be distributed to 6.0 quenches in the average coil from the DDQ package, 3.64 quenches from a coil in a DSQ package, and 2.7 quenches from a coil in an OSQ package. The average qualifying current for the various packages are 58.4 amperes for the OSQ package, 55.3 amperes for the DSQ packages, and 56.5 amperes for the DDQ package.

The heat load data is summarized in Table IV.

Table IV

Spool Heat Load (Watts) at 4.2K, with a Lead Tower Gas Flow of 32 cfh helium (STP)

TSA - 3.2± .5 watts
TSB - 5.3± .5 watts
TSC - 5.3± .5 watts
TSD - 7.4± .5 watts
TSE - 5.3± .5 watts
TSF - 7.4± .5 watts
TSH - 11.2± 1.0 watts*

*(This is with a 5kA power lead gas flow of 266 cfh helium (STP) for the pair [0.374 g/sec]).

The energy loss/cycle for a typical correction coil measured electrically[6] is approximately 17 joules where less than a fraction of a joule can be accounted for by eddy current loss[7].

The correction coil packages are installed in the accelerator with the magnetic center on the beam axis and the upstream quadrupole field perpendicular to the "x" (horizontal) axis. This is called the ring coordinate system and all harmonics and coil angles have been transformed into this system. Note that in transforming the harmonics to the ring system, it is

assumed that all the harmonics above octupole are zero except for the dipole coil where poles up to decapole are considered.

Figures 9-41 contain histograms of the various harmonics for each correction coil type. The title gives the primary pole, the harmonic number and whether it is skew or normal. All data is in the ring coordinate system. For instance, Figure 23 is the normal octupole harmonic of the quadrupole coil.

All of the coils that have the same dimensions are grouped together. In particular, this included the two different length sextupole coils. In this case, the harmonic amplitudes are different, but their harmonic moments are the same.

Some of the coils are mounted in the skew position and some in the normal position. Thus, in the ring coordinate system, a skew quadrupole will have 100% skew quadrupole (since $G_S G_P = 1$) and almost zero normal quadrupole. Since both types of quads are grouped together, one would expect a peak at 1 for the skew quadrupole moment from the skew quadrupole coils, and a peak at zero from the normal coils, as shown in Figure 20. Figure 19 shows the reverse case. This effect can also be seen in Figures 41 and 42. The Dipoles have a -0.2% decapole component due to their geometry. Therefore, skew Dipoles will have a -0.2% skew component and normal ones will have zero skew component.

As mentioned above, the correction element packages are centered on the sextupole. Since the center of the sextupole is defined as the point where the magnetic field is zero, the quadrupole field will be identically zero.

Figures 43-48 are the histograms of the angles of the various coils with respect to the quadrupole coil. Thus Figures 43 and 45 give the relative alignment of the coils in a Dipole-Sextupole-Quadrupole package. Figure 46 gives the relative alignment of the upstream and downstream packages. The large angles are from early production runs before an electronic alignment system was installed.

Acknowledgements

The Engineers and technical people who constructed the spools in such a timely fashion with great care under the direction of Mr. D. Smith and enabled this data to be obtained - a vote of thanks.

References

1. M. Kuchnir, R. J. Walker, W. B. Fowler, and P. M. Mantsch, IEEE Transactions on Nuclear Science, (1981), Vol. NS-28, No. 3, p. 3325.
2. D. Ciazynski, P. Mantsch, IEE Transactions on Nuclear Science, (1981), Vol. NS-28, No. 3, p. 3275.
3. A. D. McInturff, M. Kuchnir, & P. Mantsch, "Cryogenic Correction Coil Testing", 1983 Particle Accelerator Meeting Proceedings, Santa Fe, New Mexico
4. R. Shafer, Private Communication (Internal Memo), Fermi National Accelerator Laboratory, (1981).
5. R. Shafer, "Eddy Currents, Dispersion Relations and Transient Effects in Superconducting Magnets", Technical Memo 991, Fermi National Accelerator Laboratory, September, 1980.
6. A. D. McInturff, D. Gross, IEEE Transactions of Nuclear Science, (June, 1981) Vol. NS-28, No. 3, p. 3211.
7. R. Shafer, Private Communication (Internal Memo), Fermi National Accelerator Laboratory, January, 1982.

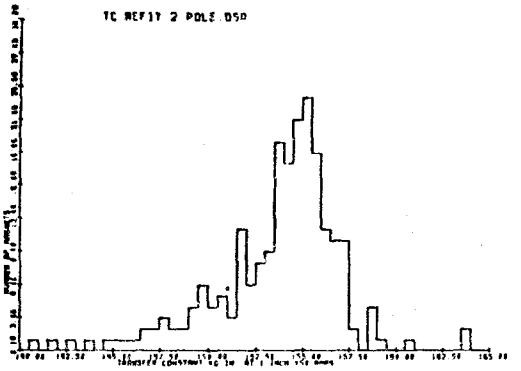

Figure 1: ∫Bdl - Dipole DSQ Package

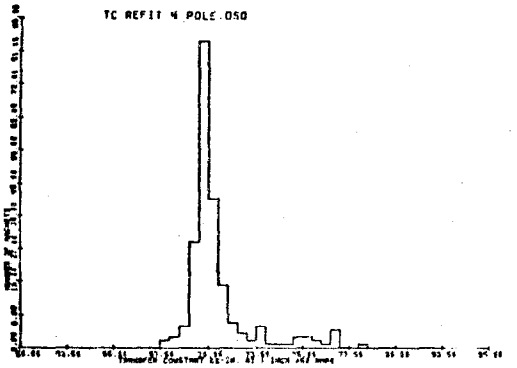

Figure 2: ∫Bdl - Quadrupole (1 in.) DSQ Package

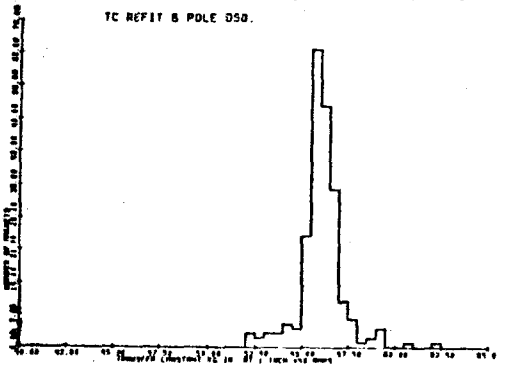

Figure 3: ∫Bdl - Sextupole (1 in.) DSQ Package

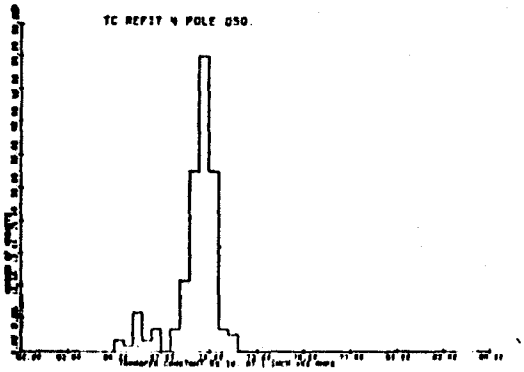

Figure 4: ∫Bdl - Quadrupole (1 in.) OSQ Package

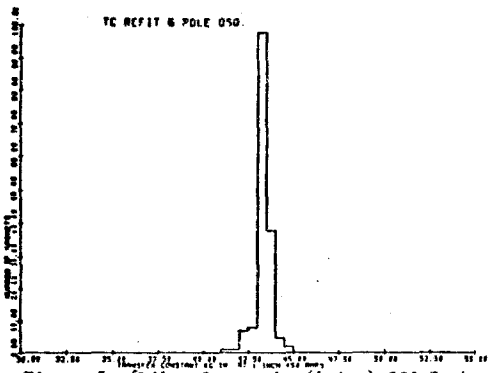

Figure 5: ∫Bdl - Sextupole (1 in.) OSQ Package

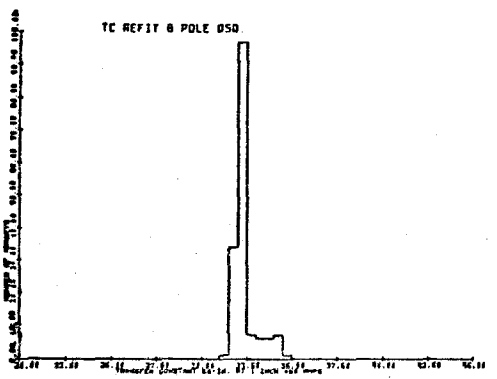

Figure 6: ∫Bdl - Octupole (1 in.) OSQ Package

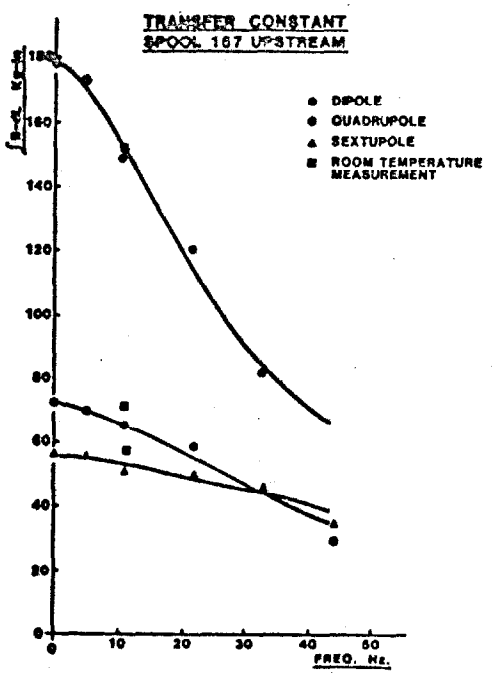

Figure 7: ∫Bdl - 4.2K DSQ Package

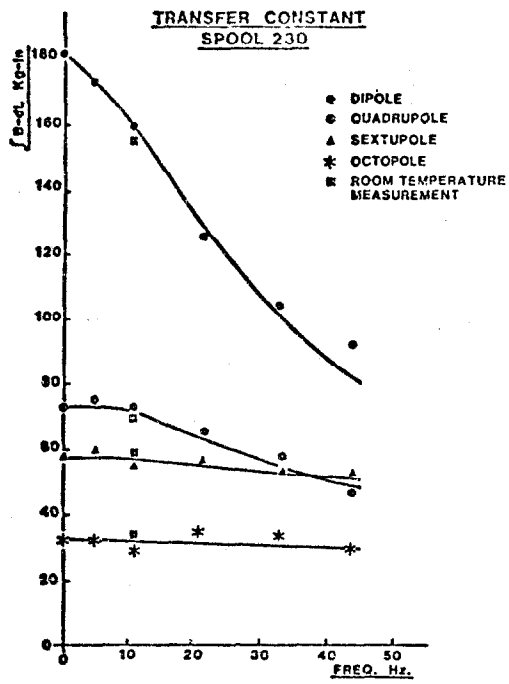

Figure 8: ∫Bdl - 4.2K - Both Packages

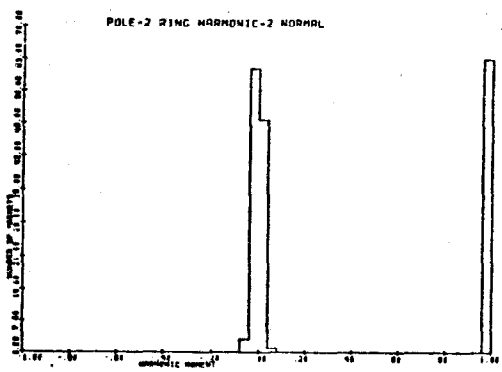

Figure 9: Dipole moment of dipole

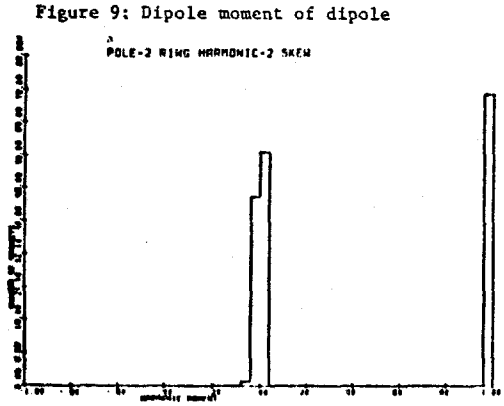

Figure 10: Skew Dipole moment of the dipole

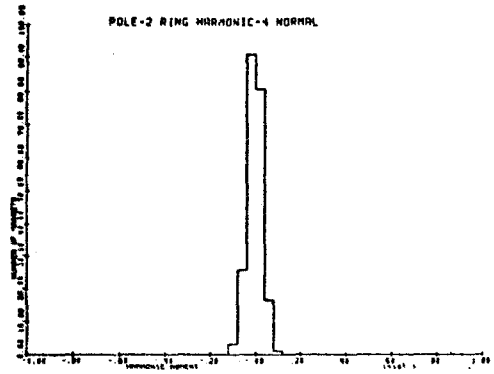

Figure 11: Quadrupole moment of the dipole

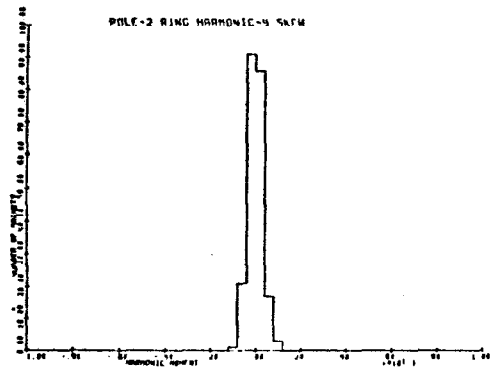

Figure 12: Skew quadrupole moment of the dipole

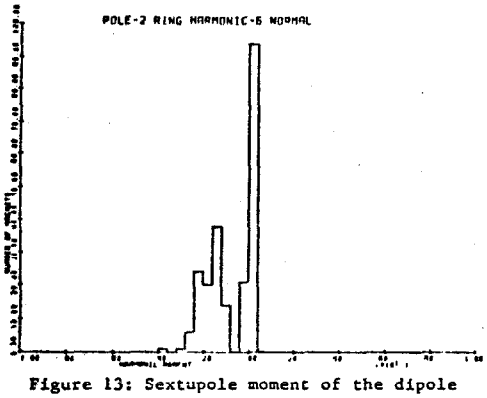

Figure 13: Sextupole moment of the dipole

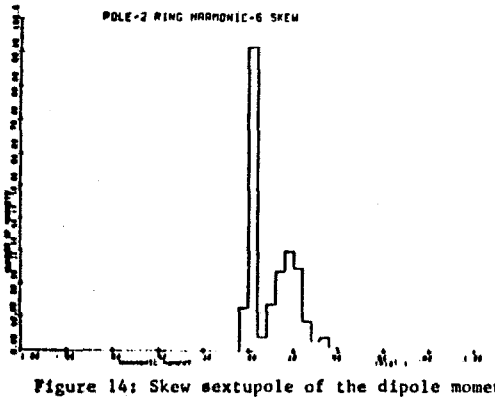

Figure 14: Skew sextupole of the dipole moment

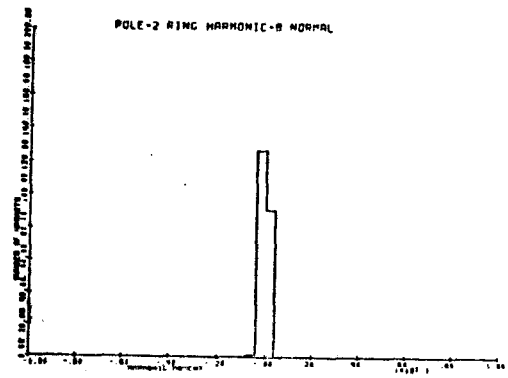

Figure 15: Octupole moment of the dipole

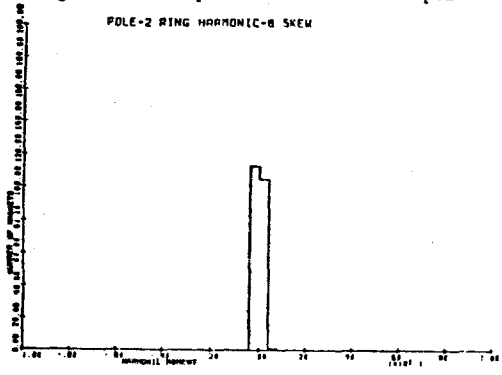

Figure 16: Skew octupole moment of the dipole

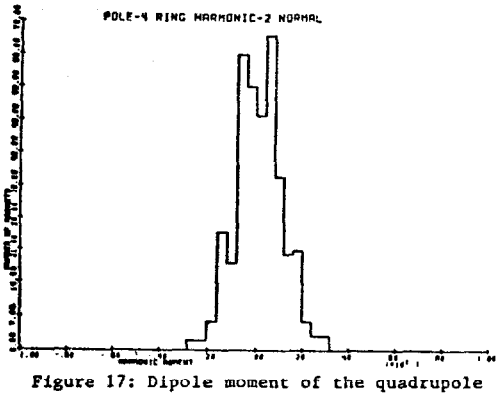

Figure 17: Dipole moment of the quadrupole

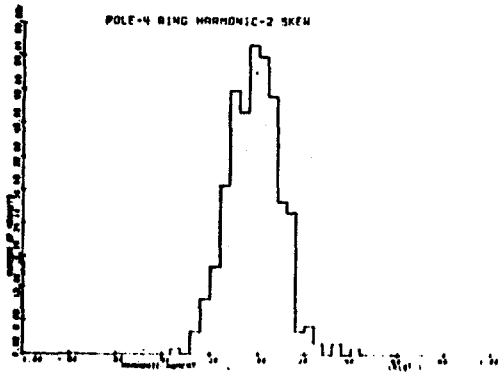

Figure 18: Skew dipole moment of the quadrupole

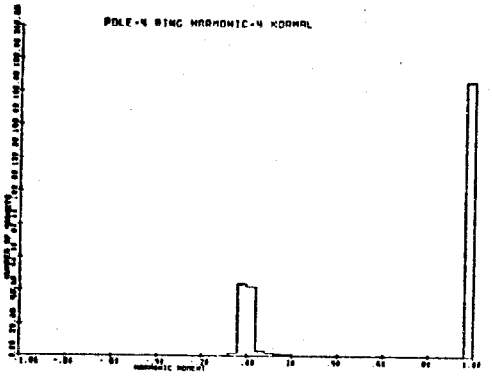

Figure 19: Quadrupole moment of the quadrupole

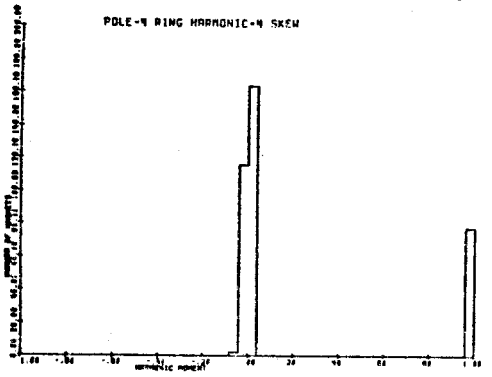

Figure 20: Skew quadrupole moment of the quadrupole.

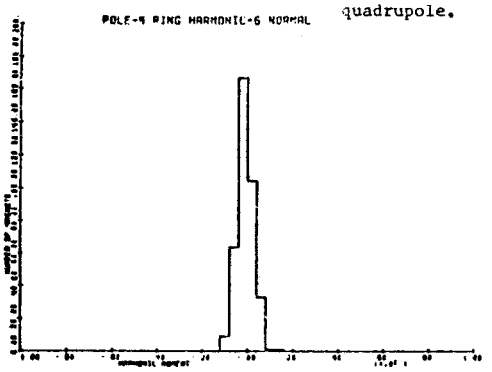

Figure 21: Sextupole moment of the quadrupole

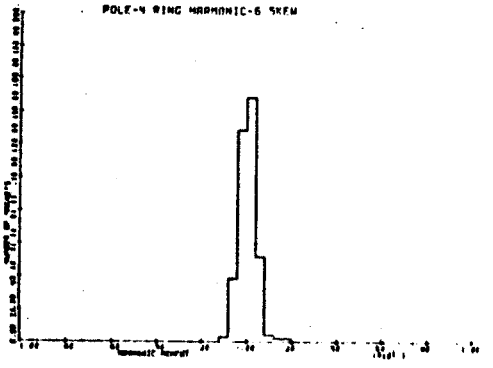

Figure 22: Skew sextupole moment of the quadrupole

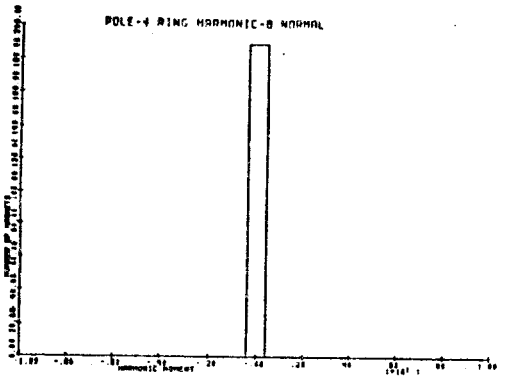

Figure 23: Octupole moment of the quadrupole

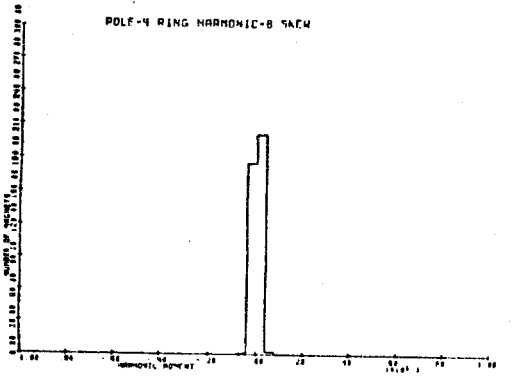

Figure 24: Skew octupole moment of the quadrupole

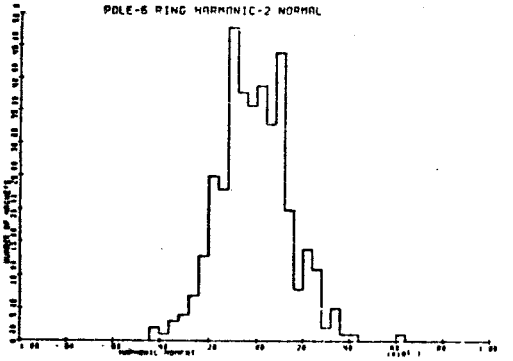

Figure 25: Dipole moment of the sextupole

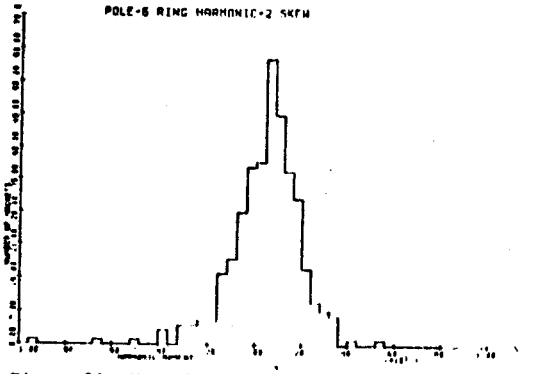

Figure 26: Skew dipole of the sextupole

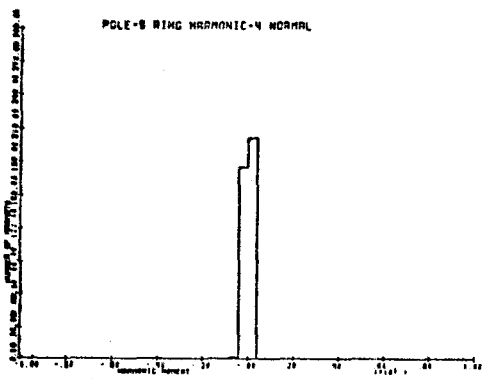

Figure 27: Octupole moment of the sextupole

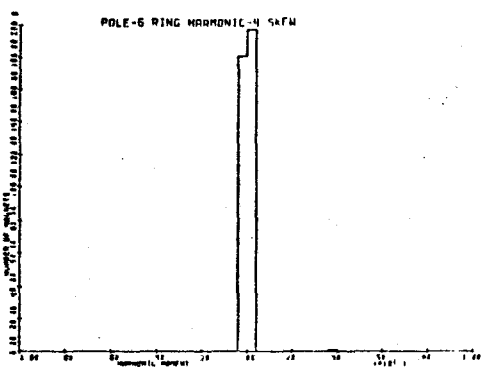

Figure 28: Skew octupole moment of the sextupole

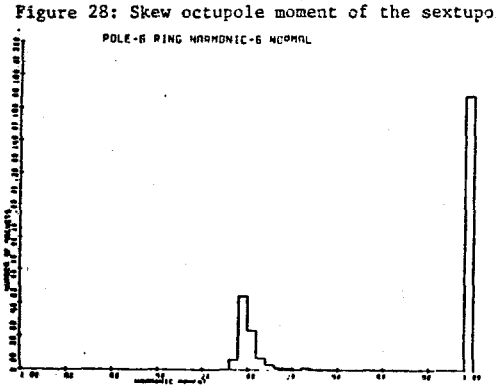

Figure 29: Sextupole moment of the sextupole

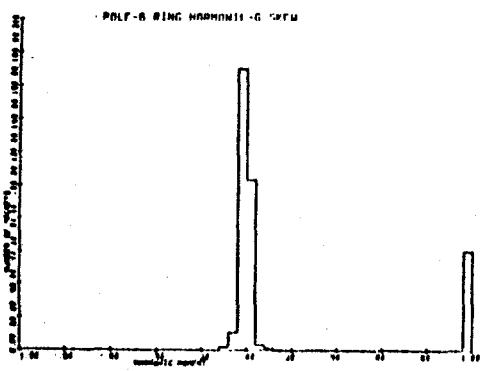

Figure 30: Skew sextupole moment of the sextupole.

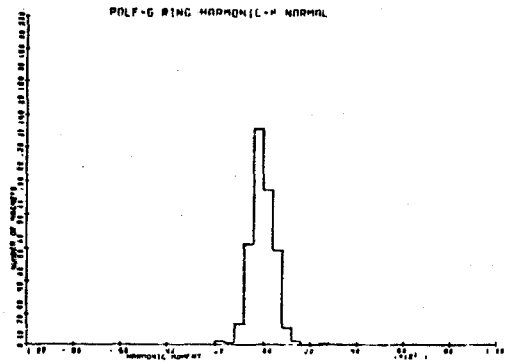

Figure 31: Octupole moment of the sextupole

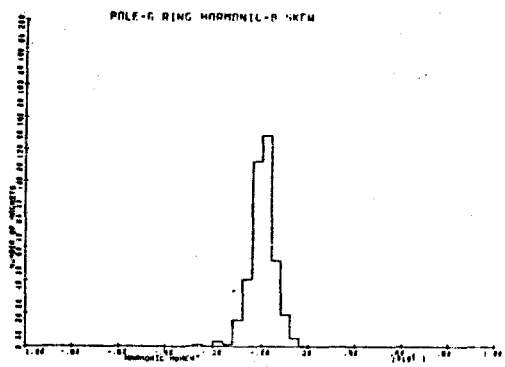

Figure 32: Skew octupole moment of the sextupole

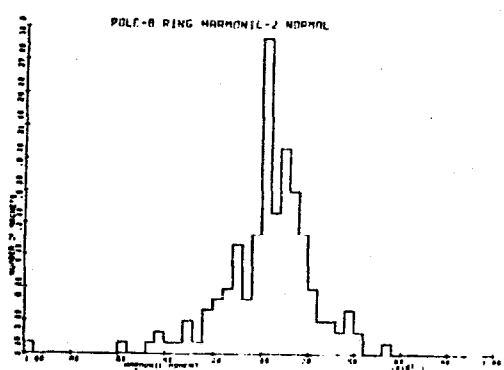

Figure 33: Dipole moment of the octupole

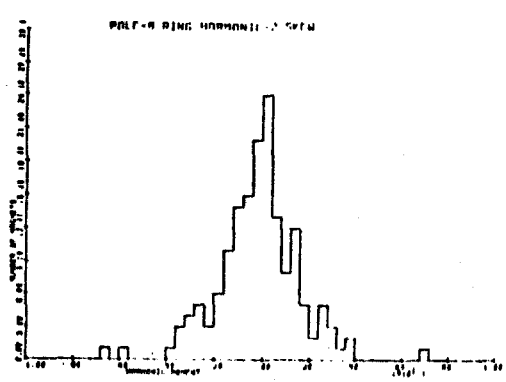

Figure 34: Skew dipole moment of the octupole

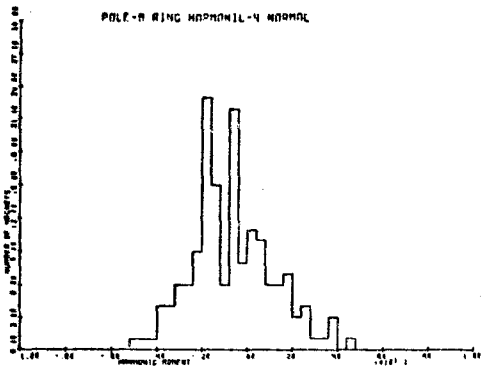

Figure 35: Quadrupole moment of the octupole

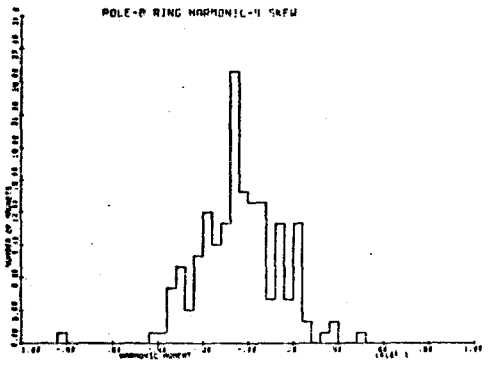

Figure 36: Skew quadrupole moment of the octupole

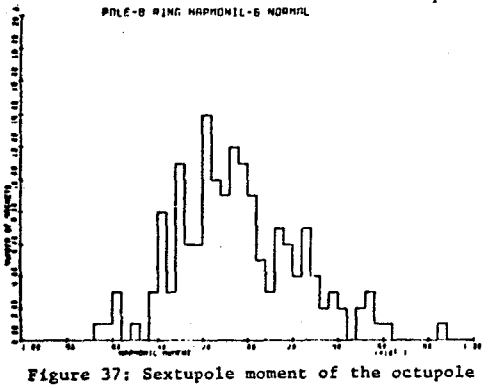

Figure 37: Sextupole moment of the octupole

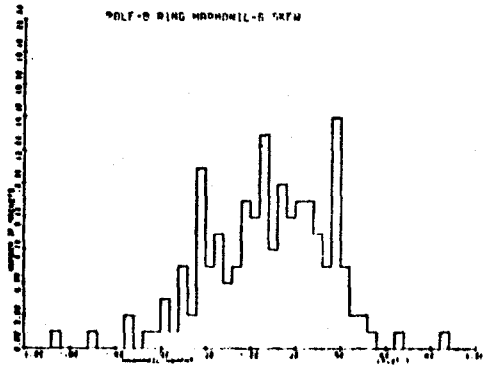

Figure 38: Skew sextupole moment of the octupole

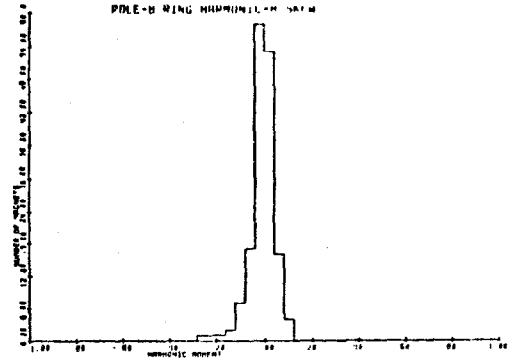

Figure 39: Skew octupole moment of the octupole

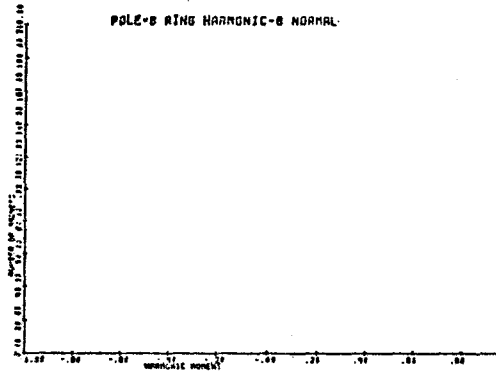

Figure 40: Octupole moment of the octupole

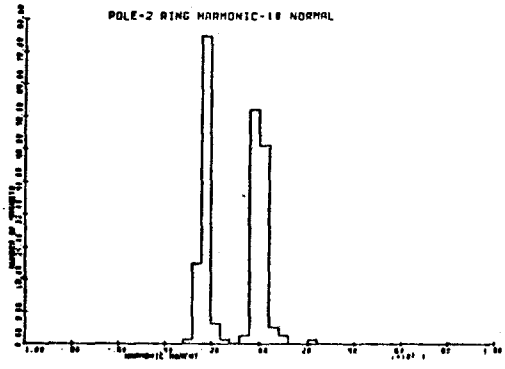

Figure 41: Decapole moment of the dipole

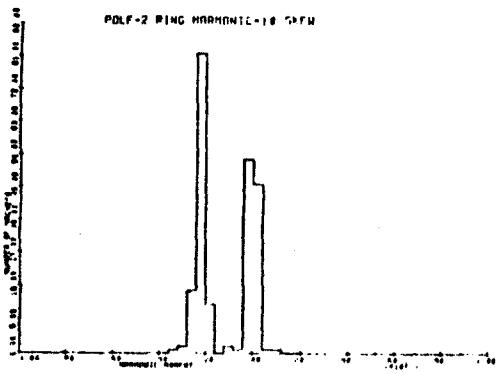

Figure 42: Skew decapole moment of the dipole

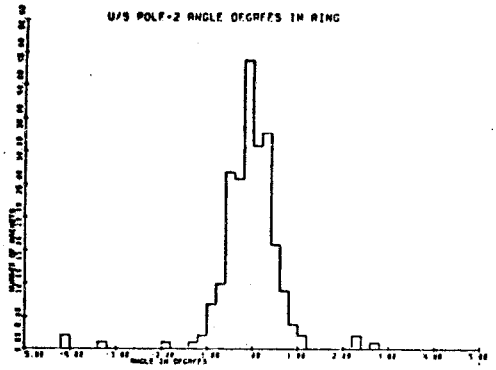

Figure 43: Upstream dipole (DSQ) angle

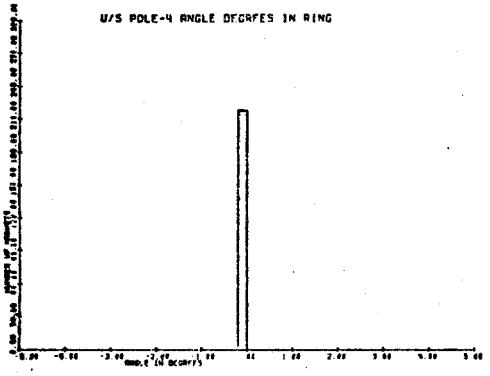

Figure 44: Upstream quadrupole (DSQ) angle

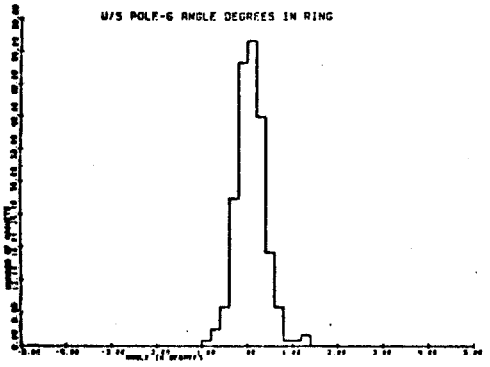

Figure 45: Upstream sextupole (DSQ) angle

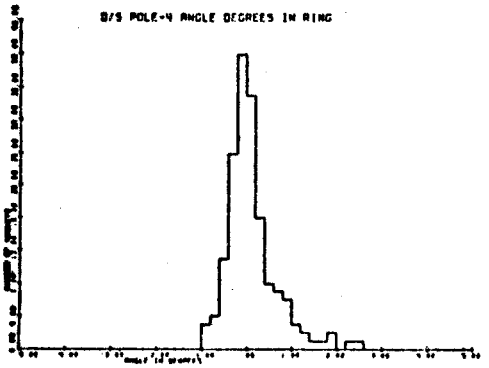

Figure 46: Downstream quadrupole (OSQ) angle

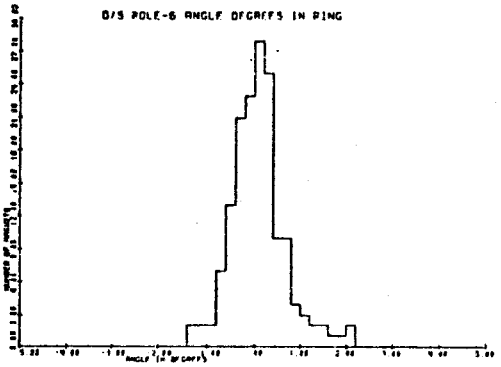

Figure 47: Downstream sextupole (OSQ) angle

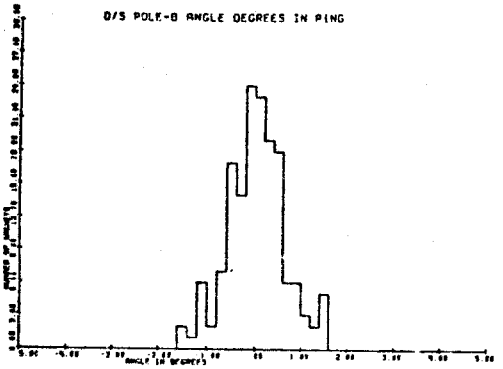

Figure 48: Downstream octupole (OSQ) angle